

# TRIBOLOGICAL MODELLING OF THE NORMAL FORCES DISTRIBUTION ON THE TOOTHED CHAIN LINKS

Mihai – Tiberiu LATES<sup>1</sup>, Radu PAPUC<sup>2</sup>, Cornel – Cătălin Gavrila<sup>3</sup>

<sup>1</sup> Transilvania University of Brasov, [latesmt@unitbv.ro](mailto:latesmt@unitbv.ro)

<sup>2</sup> Transilvania University of Brasov, [radu.papuc@unitbv.ro](mailto:radu.papuc@unitbv.ro)

<sup>3</sup> Transilvania University of Brasov, [cgvavrila@unitbv.ro](mailto:cgvavrila@unitbv.ro)

**Abstract**—This paper deals with the mathematical modelling of the normal forces distribution and of the contact pressure between the chain and the tensioning guide. In the first step, using Hertz theory, it is performed, for two cases, the modelling of normal forces distribution on the geared chain straps that are in contact with the guide. At the end there are presented the conclusions about pressure variations in the contact area between the guide and the chain.

**Keywords**— Hertz, Von Mises Stress, tooth chain, pressure, tensioning guide, guiding sprockets links, interior link, exterior link.

## I. INTRODUCTION

THE functioning of all mechanical systems, from the most common ones to the more complex, assume the existence of interactions between elements found in relative motion [1].

From the mechanical point of view, but also from the motion point of view, an interaction assumes developing forces and moments which allow transmitting power from one element to another, ensuring the normal functioning of the whole system. In the mean time, any interaction will have an energy lost through friction, which will manifest at a surface level between elements found in interaction, as well as a deterioration source of the surfaces found in contact, by developing complex wear processes [2]-[5].

The chain transmissions are part of the indirect mechanical transmissions and serve at motion transmission and torsion moment between two or more parallel axes [6].

## II. MODELLING THE CHAIN- GUIDE ENSEMBLE WITH FINITE ELEMENTS

Using the CATIA v5 R19, the geometrical model can be achieved. Every component is modelled as a different part. The final assembly can be obtained by taking into account the contact of geometrical constraints between

the guide and the links.

This assembly is imported as geometry in the ANSYS 15.0 software.

The finite elements method (FEM) is a numerical method used to solve equations with partial derivatives of physical systems with an infinite number of freedom degrees [7], [8].

By applying this method, these equations with partial derivatives are reduced to systems with algebraic equations, meaning to a discrete system with a finite number of freedom degrees [9].

In Fig. 1 is presented the model of a guide chain ensemble, which highlights the elements that are treated in this study.

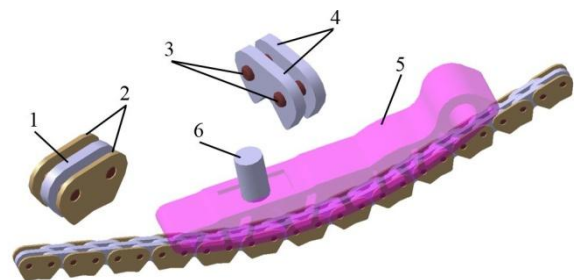


Fig.1. Guide - chain ensemble:

1- interior link; 2- guiding sprockets links; 3- bolts; 4- exterior link; 5- tensioning guide; 6- pressure elements.

The numerical evaluation is made on two models connected on a geared chain in order to determine the distribution of pressures in the contact zones.

The two models differ by guide radius and have the same value of the guide arrow towards the chain.

Considering the two arrows of the guide, the number of chain links in contact with the guide differ as following:

- 1) to the guide with the radius of 100 (mm) corresponds a medium number of links in contact  $n_z = 6.5$ ;
- 2) to the guide with the radius of 150 (mm) corresponds a medium number of links in contact  $n_z = 7.5$ .

The normal force applied to the models is  $F_n = 58$  (N).

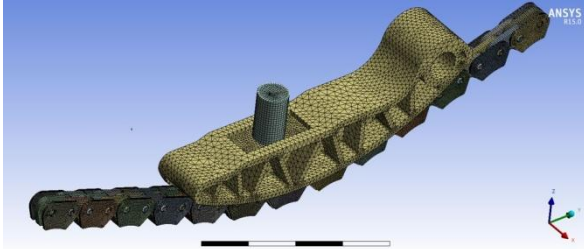


Fig. 2. Meshing model A.

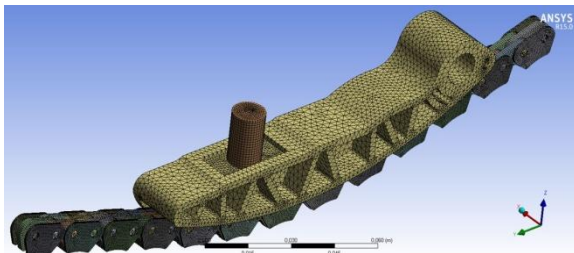


Fig. 3. Meshing model B.

In Fig. 2 and Fig. 3 there are presented the models which will be analysed:

- 1) model A – guide radius  $R = 100$  (mm);
- 2) model B – guide radius  $R = 150$  (mm).

The links are made from steel with the following properties [10]:

- 1) Young module  $E=200000$  (MPa);
- 2) Tensile Yield Strength  $\sigma = 250$  (MPa);
- 3) Ultimate Strength  $\sigma_r = 460$  (MPa);
- 4) Density  $\rho = 7850$  ( $kg \cdot m^{-3}$ );
- 5) Poisson coefficient  $\nu=0.3$ .

The guide is made by a PAX type polyamide with the mechanical properties as [11]:

- 1) Young module  $E=2800$  (MPa);
- 2) Tensile Yield Strength  $\sigma = 38$  (MPa);
- 3) Density  $\rho = 1.29 \cdot 10^{-9}$  ( $kg \cdot m^{-3}$ );
- 4) Ultimate Strength  $\sigma_r = 70$  (MPa);
- 5) Poisson coefficient  $\nu=0.42$ .

The material properties are used in the finite elements modelling of the two ensembles (tensioning guide - geared chain) and the results are presented in the following steps.

### III. CONTACT PRESSURES STUDY

The loading mode of the two models and the imposed boundary conditions are presented in Fig. 4 where  $F_n$  was applied normally to the pressure element surface, the chain was fixed at both ends with none freedom degrees and for the guide there were restricted five freedom degrees, allowing the transition only about the z-axis. In the Fig. are highlighted the contact zones defined in ANSYS software.

The static characteristic for these models, as well as the results of the modelling are presented in the next steps. Because of the force which is applied to the A

model, it is obtained a theoretical distribution which has a uniform distribution. The result of the maximum displacement is from 0,0177 (mm).

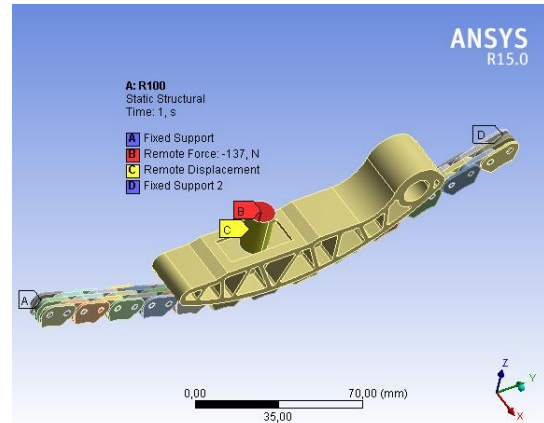


Fig. 4. The finite element model

The distribution of the displacements  $s$  is shown in Fig. 5.

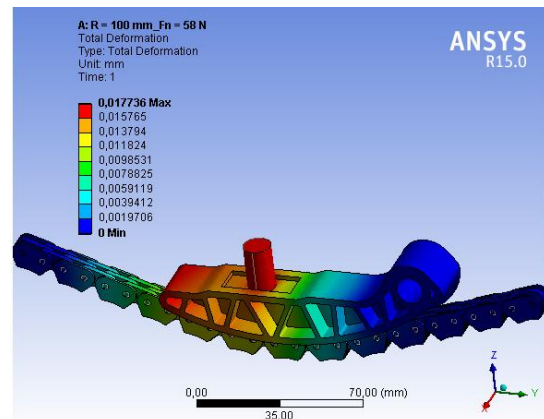


Fig. 5. Displacement distribution

Fig. 6 shows the Von Mises stress distribution. On the links is a maximum distribution with values accepted of  $\sigma = 300$  (MPa). A maximum of 9.827 (MPa) is acceptable – the pressures appeared between links and guide.

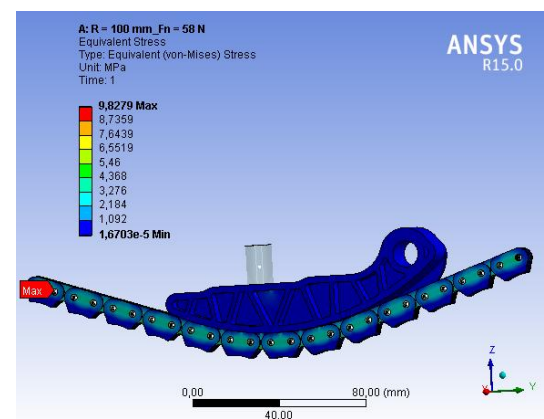


Fig. 6. Von Mises Stress.

The distribution of the contact pressure between the guide with the radius  $R = 100$  (mm) and the geared chain links is represented in the Fig. 7.

From the Fig. it is observed that the maximum pressure of 2.468 (MPa) was found in the action area of the normal force applied to the guide.

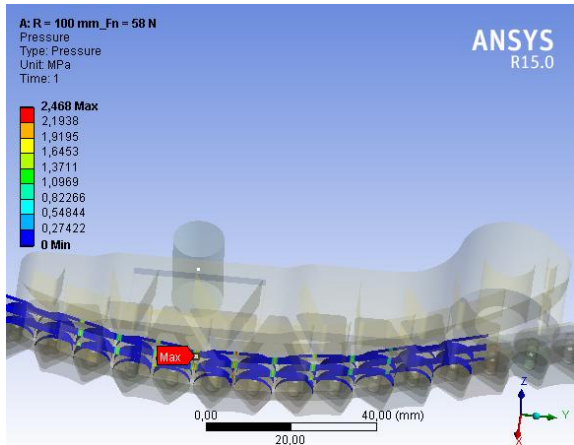


Fig. 7. Pressure distribution for  $R = 100$  (mm) and  $F_n = 58$  (N)

The results of the analyse for the case B, are presented below.

Because of the force which is applied to the B model, is obtained a theoretical distribution which has a uniform displacement from 0.0224 (mm) – Fig. 8.

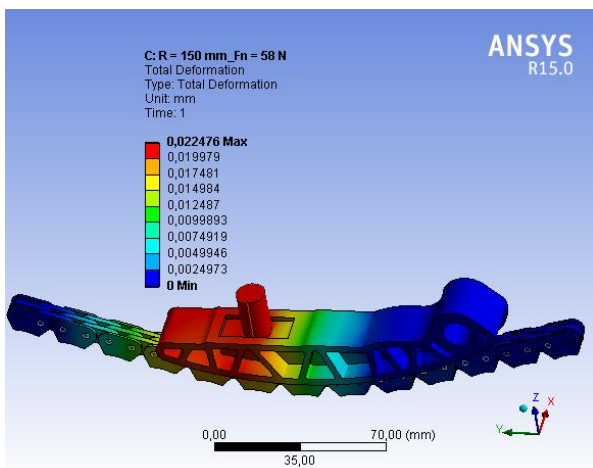


Fig. 8. Displacement distribution

Fig. 9 shows the Von Mises stress distribution. A maximum of 11.272 (MPa) is acceptable – the pressures appeared between links and guide.

The pressure distribution in the contact zones between the guide with the radius of  $R = 150$  (mm) and the geared chain links is highlighted in the Fig. 10 – the maximum value is 2.340 (MPa).

In order to determine the specific pressure, there were read the obtained values on each link found in contact with the tensioning guide.

In Fig. 11 it is presented the position of the links in

contact with the tensioning guide profile (where  $l$  is the distance that defines the link's position in contact with the guide, and  $p$  is the chain step).

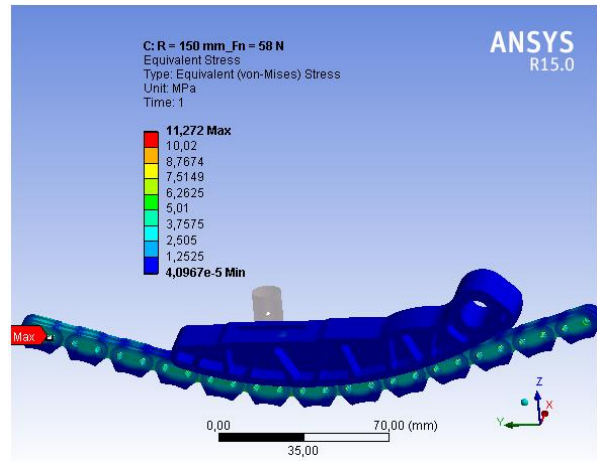


Fig. 9. Von Mises Stress.

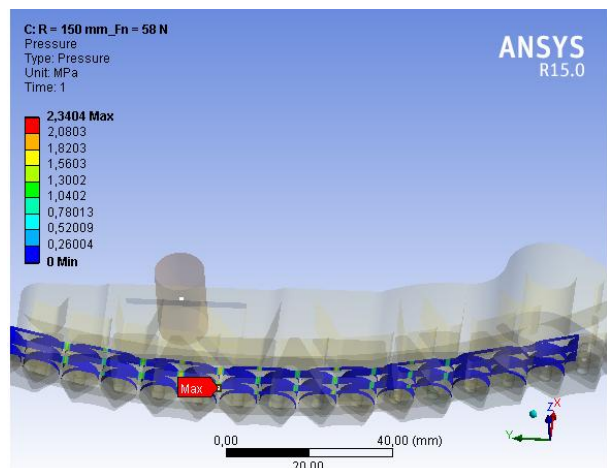


Fig. 10. Pressure distribution for  $R = 150$  (mm) and  $F_n = 58$  (N)

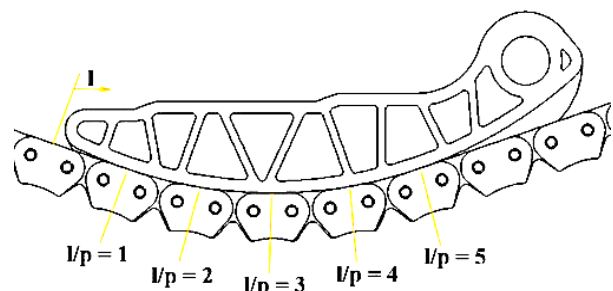


Fig. 11. Position of the link in contact with the guide profile with the radius  $R = 100$  (mm)

The obtained results allowed determining the variation diagrams of the contact pressures regarding the link position in contact with the guide profile. In the case when the guide radius is  $R = 100$  (mm) it can be observed that the pressure is maximum in the action zone of the normal force applied to the guide; this is shown in

Fig. 12 and Fig. 13.

--- Guiding sprockets links\_ Interior links\_Fn = 58 (N)

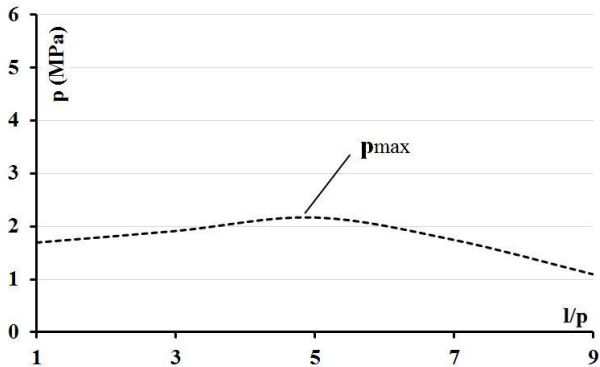


Fig. 12. The contact pressures variation considering the link position  $l/p$  and the stress force, for  $R = 100$  (mm) in the case of guiding and interior links.

--- Exterior links\_Fn = 58 (N)

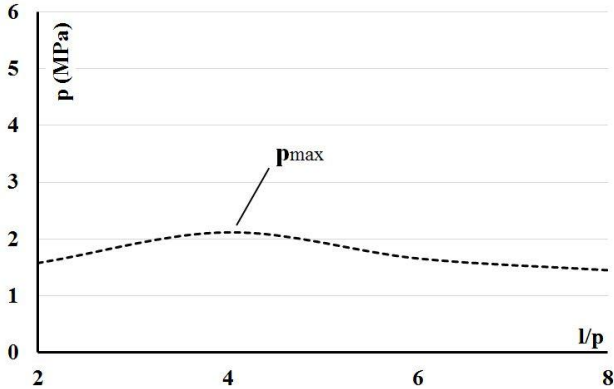


Fig. 13. The contact pressures variation considering the link position  $l/p$  and the stress force, for  $R = 100$  (mm) in the case of exterior links.

From the Fig. 14 and Fig. 15, where the guide radius is  $R = 150$  (mm), it is observed the tendency of a maximum local pressure appearance; this is due to the friction forces between links and guide.

--- Guiding sprockets links\_ Interior links\_Fn = 58 (N)

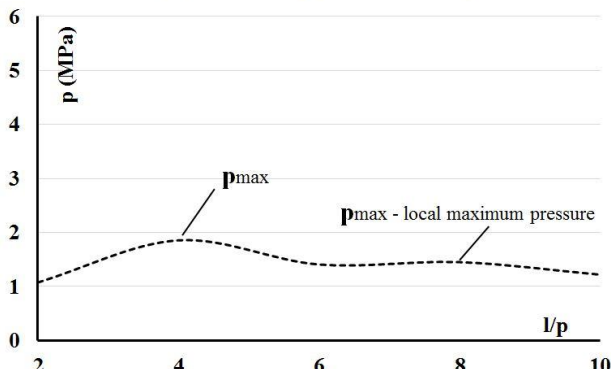


Fig. 14. The contact pressures variation considering the link position  $l/p$  and the stress force, for  $R = 150$  (mm) in the case of guiding and interior links.

The diagrams from Fig. 14 and Fig. 15 show that on the link moving along the guide, the pressure crosses at least one pressure peak having the tendency of having another supplementary peak for longer guide contact lengths, this suggesting a dynamic character of the phenomena produced in the guide-link contact.

--- Exterior links\_Fn = 58 (N)

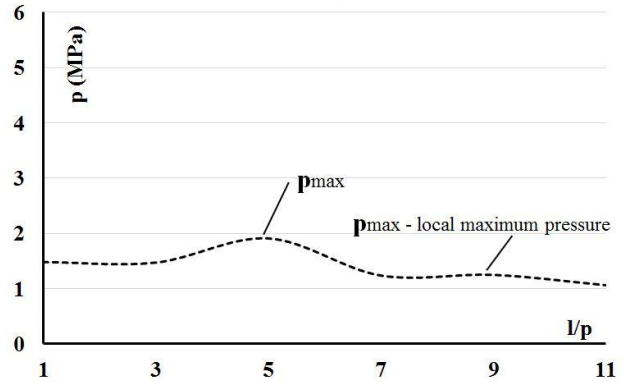


Fig. 15. The contact pressures variation considering the link position  $l/p$  and the stress force, for  $R = 150$  (mm) in the case of exterior links

To describe the tribological link - guide contact, the necessary parameter is the normal force and not the maximum pressure determined after the simulations presented previously, simulations that consider the contact between solids.

The Hertz model for the solids contacts offers the correspondence between the maximum pressure between contact and the normal force which determines it.

The form of the two contact surfaces is shown Fig. 16.

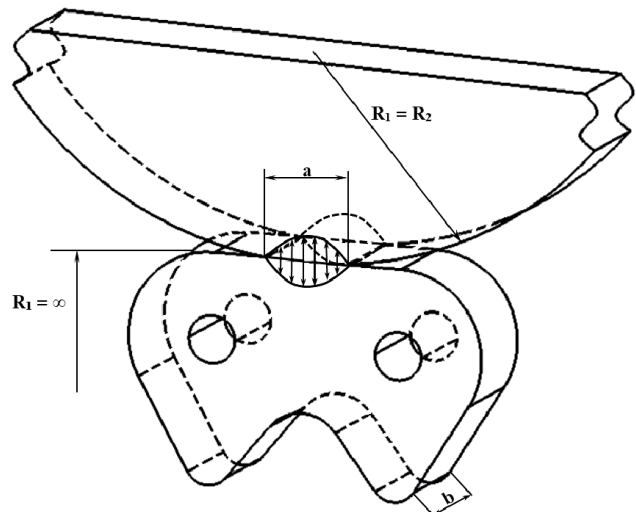


Fig. 16. The form of the contact surfaces

In the case of the guide and the geared link, with the radius  $R_1 = R$ , respectively  $R_2 = \infty$ , the contact length is calculated with the relation [12]

$$a = \sqrt{\frac{4 \cdot F \cdot R}{\pi \cdot b \cdot E}} \quad (1)$$

In the relation (1), F is the normal force on the geared links in contact with the guide profile and is determined with the relation:

$$F = \pi \cdot a \cdot b \cdot p_{\max} \quad (2)$$

where: R represents the guide radius; b - width of the link;  $p_{\max}$  - maximum pressure on the geared link;  $E_{\text{red}}$  - the reduced Young model on the two elements in contact. This is determined by the relation:

$$\frac{1}{E} = \frac{1}{2} \cdot \left( \frac{1 - \nu_1^2}{E_1} + \frac{1 - \nu_2^2}{E_2} \right) \quad (3)$$

where:  $\nu_1 = 0.42$  is the Poisson coefficient for the guide material (polyamide PAX);  $\nu_2 = 0.3$  - Poisson coefficient for the geared link material (steel);  $E_1 = 2.5 \cdot 10^{-4}$  - the reduced Young model for the guide material;  $E_2 = 4.55 \cdot 10^{-6}$  - the reduced Young model for the geared link material [13]-[16].

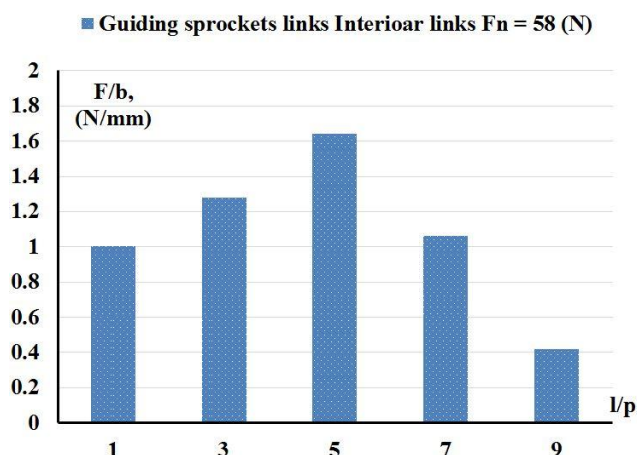


Fig. 17. The specific normal forces on the guiding sprockets and interior links with the link's position l/p and the pressure force, for the guide radius R = 100 (mm)

In the Fig. 17 and 18 are represented the specific normal forces on the guiding links, interior and exterior, depending on the link's position l/p, for the force  $F_n$  applied to the guide with the radius R = 100 (mm).

From the two diagrams it can be observed that on some geared links, the specific normal forces are big. This aspect can be explained because in those zones acts the force  $F_n$  applied to the guide.

The diagrams from the Fig. 19 and 20 present the specific normal forces on the guiding links, interior and exterior, depending on the link's position l/p, for the three pressure forces applied to the guide with the radius

R = 150 (mm). Like in the previous case, the specific normal forces on the geared links are bigger in the zones where the pressure forces act on the guide.

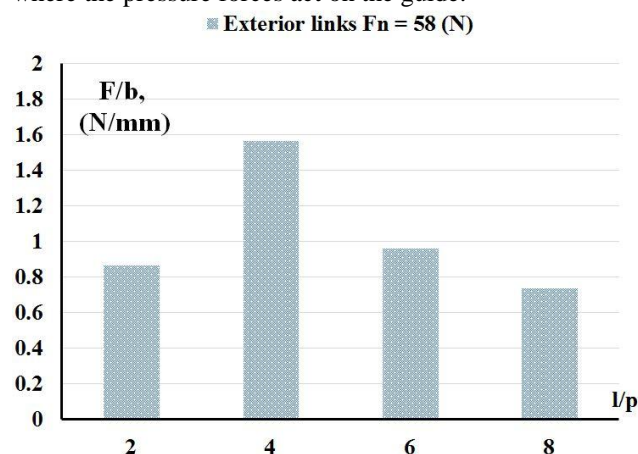


Fig. 18. The specific normal forces on the exterior links depending on the link's position l/p and the pressure force, for the guide radius R = 100 (mm)

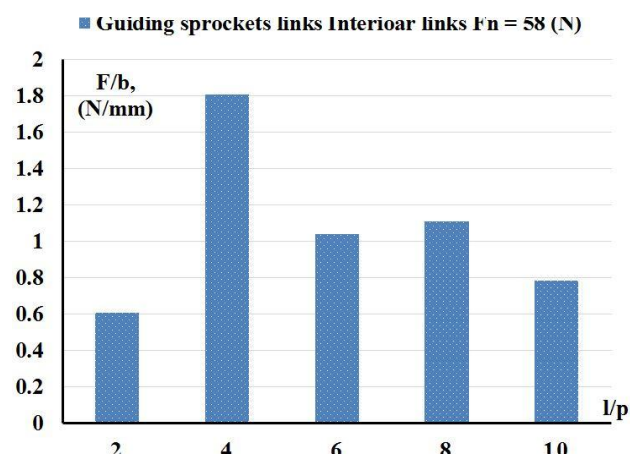


Fig. 19. The specific normal forces on the guiding and interior links depending on the link's position l/p and the pressure force, for the guide radius R = 150 (mm)

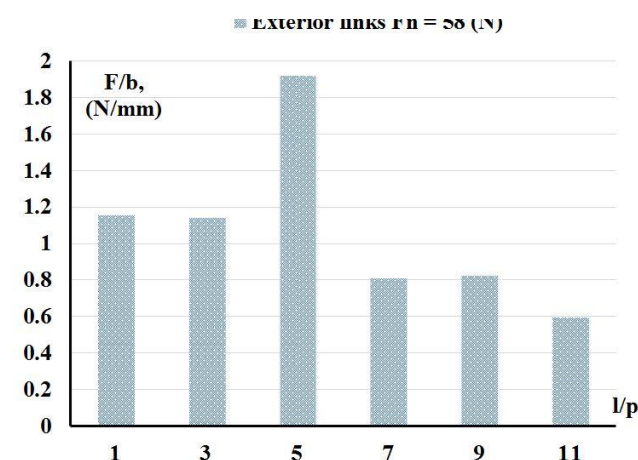


Fig. 20. The specific normal forces on the exterior links depending on the link's position l/p and the pressure force, for the guide radius R = 150 (mm)

Based on diagrams shown in Fig. 10 and 11 it can be concluded that the force depends on the width of the links in contact with guide profile.

#### IV. CONCLUSION

The optimal design of the guide chain system should follow the achieving of the fluid friction condition in the wide domain into a functional operating regime of the engine with internal combustion [17], [18].

For a guide - chain contact with small contact pressures the aim is to increase the number of the links in contact with the guide. The number of the links in contact with the guide depends on the mounting rise and on the guide's radius.

By increasing the mounting rise the pushing forces will be increased which influences negatively the transmission's efficiency; so, the only way to increase the contact links number is to increase the guide's radius.

The static analysis of the guide – chain contact pressures indicates that one maximum value of the contact pressure is placed in the area where the pushing force is applied to the guide.

By increasing the guide's radius and the number of the contact links a supplementary local maximum value of the contact pressure appears. The contact pressures values are decreasing with the increasing of the guide's radius.

The von Mises maximum stresses for the two cases are situated in articulated areas of the toothed chain. The maximum tension was obtained in the articulated end area of the chain.

From the critical analyse of the specific normal forces applied on the interior and exterior guiding sprockets links, in contact with guide profile, it can be observed:

- 1) *The maximum specific normal forces have the value up to 2 (N/mm).*
- 2) *It does not exist the main difference regarding the normal force in the contact between the guide and the different links.*
- 3) *For an increased value of the guide's radius, the contact pressure has two local maximum values; this indicates the possibility of appearing the resistance to the lubricant expulsion from the contact area which is important in order to maintain the lubricant film.*
- 4) *The pressure distribution is influenced by the construction of the chain guide pressing system and at the same time it depends on from the contact geometry materials and guide geometry*

Considering the analysis and the results reading regarding the theoretical distribution of the displacement of the two cases analysed, it can be concluded that the maximum stress is in the zone where the normal force is applied to the guide pressure element.

From the comparative analysis of the pressures variation on the guiding and interior links for the two

cases it is observed that once the guide radius grows, the pressures tend to decrease, this being related to the corresponding growth of the medium number of links in contact with the guide profile.

#### REFERENCES

- [1] D. N. Reshetov, "Machine design", Ed. Mir Publisher, Moscow, 1978, pp. 411-436.
- [2] R. Velicu, M. T. Lates, s.o., "Theoretical and experimental study of friction in bearing mountings", VII Iberian Conference on Tribology, FEUP, Porto, Portugal, 20-21 June, 2013, pp.1-6.
- [3] M. Lates, A. Jula, "Machine elements and mechanical transmission, Organe de masini si transmisii mecanice", Ed. Universitatii Transilvania, Brasov, 2005.
- [4] H. Roloff, W. Matek, s.a., "Machine elements, Organe de masini", Ed. Matrix Rom, Bucuresti, vol. 2, 2008, pp. 652-668.
- [5] X. War, A., Dwyer-Joyce, R. S., "Model Experiments on Automotive Chain Drive Systems", Elsevier Science, Vol 39, p 851-861, 2001.
- [6] J. Vlasnik, "Chain drive computational model as virtual engine module", Ph.D. Thesis. Brno University of Technology, Česká Republika, pp. 7-87, 2009.
- [7] L. L., Kent, "Structural and thermal analysis using the Ansys Workbench release 14 environment", Ed. Stephen Schroff, 2012.
- [8] O.C. Zienkiewicz and R.C. Taylor, "The finite element method", 6th Edition, Elsevier, 2006.
- [9] P.K. Goenka, "Dynamically Loaded Journal Bearings: Finite Element Method Analysis", Trans. ASME Ser. F, Journal of Tribology, vol. 106, pp. 429-439, 1984.
- [10] B. Mouhmid, A. Imad, N. Benseddiq, D. Lecompte, "An experimental analysis of fracture mechanisms of short glass fibre reinforced polyamide 6,6 (SGFR-PA66)", Composites Science and Technology, vol. 69, Elsevier, pp. 2521-2526, 2009.
- [11] M. De Monte, E. Moosbrugger, M. Quaresimin, "Influence of temperature and thickness on the off-axis behaviour of short glass fibre reinforced polyamide 6.6 – Quasi-static loading", Journal of Composites, Part A, No.41, pp. 859-871, 2010.
- [12] F. G., Nakhatakyan, "Precise Solution of Hertz Contact Problem for Circular Cylinders with Parallel Axes", published in Vestnik Mashinostroeniya, pp. 3-62011.
- [13] I., Sevostianov, M., Kachanov, "Contacting rough surfaces: Hertzian contacts versus welded areas", Springer Science Business Media B.V., 2007.
- [14] G. W. Stachowiak, A.W. Batchelor, "Engineering tribology", Ed. Elsevier, 3rd ed., Burlington, 2005.
- [15] J. Williams, "Engineering tribology", Ed. Cambridge University Press, New York, 2011.
- [16] W. Shizhu, H. Ping, "Principles of tribology", Ed. Tsinghua University Press, Singapore, 2012.
- [17] R. Velicu, M. T. Lates, "Time depending friction in bearing mountings", Current Solutions in Mechanical Engineering (ICOME 2015), Trans Tech Publications Ltd. Switzerland, pp 79-84, 2016.
- [18] R. Velicu, Design methodology for a planetary multiplier with synchronous belts or chains *Analele Universității din Oradea, Fascicula Management și Inginerie Tehnologică*, vol XI(XXI), nr. 2, 2012, p. 2.122-2.127